

Published in final edited form as:

Fly (Austin). 2010 ; 4(2): 128–136.

## ***poly* is required for nurse-cell chromosome dispersal and oocyte polarity in *Drosophila***

**Stephen Klusza and Wu-Min Deng\***

Department of Biological Science; Florida State University; Tallahassee, FL USA

### **Abstract**

During *Drosophila* oogenesis, nurse cells undergo changes in chromosomal morphology, first from the polytenic form to a transient condensed phase known as the five-blob configuration, then into a diffuse polytenic-polyploid state for the remainder of oogenesis. The mechanism by which nurse-cell chromosome dispersal is regulated remains elusive. Mutations in several genes, including the heterogeneous ribonucleoprotein genes *squid* (*sqd*) and *hrb27C*, the alternative splicing factor gene *poly U binding factor 68 kDa* (*pUf68*, also known as *half-pint*), and the germ-line-specific gene *ovarian tumor* (*otu*), that produce defects in nurse-cell chromosome dispersal also produce defects in oocyte polarity, suggesting a link between these two processes. Here, we characterize a novel gene named *poly*, which, when mutated in the germ line, disrupts nurse-cell chromosome dispersal, as well as localization of anteroposterior and dorsoventral determinants in the oocyte. We also show that *poly* interacts genetically with *hrb27C* and *otu*. We conclude that *poly* is required for nurse-cell chromosome dispersal and oocyte polarization in the *Drosophila* germ-line. In addition, our interaction data suggest that *poly* is probably a member of the characterized mRNp complex that mediates both processes.

### **Keywords**

germ-line; *drosophila*; oogenesis; nurse cell; oocyte polarity

---

*Drosophila* oogenesis serves as a versatile model for the study of spatiotemporal regulation of transcription, translation and localization of discrete mRNAs and proteins in a developmental context. The processes underlying oogenesis, from stem-cell differentiation to maturation of the oocyte, occur sequentially in long tubes called ovarioles. Each ovary includes approximately 16–20 ovarioles, and each ovariole has a germarium that contains a repository of germ-line and somatic stem cells. Germ-line stem cells self-renew and produce cystoblasts, which subsequently give rise to 15 nurse cells and 1 oocyte per egg chamber, whereas somatic stem cells produce an epithelial layer of follicle cells that covers the germ-line cells. The most prominent roles of nurse cells are the synthesis of enormous amounts of mRNAs and proteins that aid in oocyte differentiation and growth and the accumulation of maternal stockpiles of products to be used during embryogenesis.<sup>1</sup> The follicle cells communicate with the germ-line cells throughout oogenesis to support the development and differentiation of the oocyte.<sup>2</sup>

---

© 2010 Landes Bioscience

\*Correspondence to: Wu-Min Deng; wumin@bio.fsu.edu.

Authors' contributions: S.K. performed all experiments and drafted the manuscript. W.D. coordinated and supervised the experiments and helped to draft the manuscripts. Both authors read and approved the final manuscript.

The anteroposterior (AP) axis is established by localization of *oskar* (*osk*) mRNA at the posterior and *bicoid* mRNA at the anterior of the oocyte during stages 8–10 of oogenesis.<sup>3</sup> Microtubule organization plays an important role in many steps in the establishment of oocyte polarity; before stages 6–7 of oogenesis, the plus ends of the microtubules are spread throughout the nurse cells, and the minus ends are focused in the posterior of the oocyte.<sup>4</sup> In response to signaling from the posterior follicle cells, the microtubules are disassembled and renucleate, producing a reversion of the polarity of the filaments, such that the plus ends of the microtubules are oriented toward the posterior of the oocyte and the minus ends aggregate at the anterior cortex.<sup>5</sup> During stage 9, *osk* mRNA and Staufen (Stau) (a dsRNA-binding protein that colocalizes with *osk* mRNA) are both transported by Kinesin, a plus-end microtubule motor, to the posterior of the oocyte.<sup>6,7</sup> By stages 7–8, the oocyte nucleus is located at the anterodorsal corner of the oocyte, where Gurken (Grk), an EGFR ligand, is tightly localized, and is involved in dorsoventral axis polarity.<sup>8</sup> Mutations that interrupt any of these vital processes, through mutant somatic and/or germ-line cells, can potentially disrupt the AP/DV axis polarities of the oocyte.<sup>3,4,9</sup>

Recent studies have indicated that heterogeneous ribonucleoproteins (hnRNPs) such as *squid* (*sqd*) and *hrb27C*, the alternative splicing factor *poly U binding factor 68 kDa* (*pUf68*, also known as *half-pint*), and the germ-line-specific gene *ovarian tumor* (*otu*) are required for localization of *grk* mRNA to the dorsoanterior and/or localization of *osk* mRNA to the posterior of the oocyte.<sup>10–12</sup> Intriguingly, these mutants also show chromosomal morphology defects in the nurse cells from stage 6 of oogenesis onward. Nurse cells undergo an asynchronous cell cycle regimen comprising 10–12 endocycles of continuous DNA replication before programmed cell death. After the first five endocycles, the DNA coalesces visibly into the characteristic five-blob structure during stages 4–5 of oogenesis. Each blob represents one of the major polytenic chromosomal arms (X, 2L, 2R, 3L and 3R). Evidence supports the hypothesis that a transient mitosis-like phase follows the fifth endocycle, during which the polytene chromosomes disperse throughout the nurse-cell nucleus, resulting in a loss of the visible five-blob structure in all nurse cells by stage 6 of oogenesis.<sup>13</sup> Many of the mutants in which the nurse-cell chromosomes fail to disperse after the five-blob stage also show defects in localization of AP and DV axis determinants, but determination of a functional relationship between this chromosome-dispersal event and formation of the AP/DV axis polarities has been elusive. Nurse-cell chromosome dispersal has been suggested to facilitate rapid ribosomal synthesis of proteins needed for the remainder of oogenesis from stage 6 onward.<sup>13</sup>

Here we report that, from a flipase-flipase recognition-target (FLP-FRT) mosaic screen, we isolated a new allele of *poly* (*poly*<sup>2</sup>) that caused prominent defects in Stau-GFP localization and nurse-cell chromosome dispersal in germ-line clones. *poly* is a novel gene that was originally identified for the aberrant nuclear morphology it produces in the brains of third-instar larvae (Heck A, Dros Res Conf 36, Flybase; named *poly*<sup>1</sup>). We conclude that the novel gene *poly* is required for nurse-cell chromosome dispersal and oocyte polarity and suggest that *poly* can interact with members of the mRNP complex that are involved in similar processes.

## Results

*poly* is required in the germ-line for efficient Stau localization and nurse-cell chromosomal dispersal. To uncover new genes that are involved in oocyte polarity formation, we performed an FLP-FRT mosaic screen for Stau-GFP localization with approximately 400 FRT mutant lines containing P-element insertions, across the right arm of the third chromosome.<sup>14,15</sup> Stau-GFP colocalizes with *osk* mRNA at the posterior of the oocyte in wild-type stage-9 egg chambers (**Fig. 1A** and data not shown).<sup>16</sup> One of the lines that

affected the localization of Stau-GFP in egg chambers with mutant germ-line clones was *8131* (an FRT-containing P-element line from Szeged stock center); out of 66 stage-9 *8131* germ-line clones examined, 24% displayed complete mislocalization (center of oocyte; **Fig. 1B**), 53% displayed partial mislocalization (center and posterior of oocyte), and 23% retained wild-type localization (posterior of oocyte). An additional phenotype observed in *8131* germ-line clones was the alteration of nurse-cell chromosomal morphology (compare **Fig. 1C and D**). Normally, wild-type egg chambers in early oogenesis possess polytenic chromosomes that progress to a distinct five-blob configuration at stage 4, before dispersing into a diffuse state during stages 4–5. By stage 6, all of the nurse-cell chromosomes exhibit a diffuse state. The polytenic nurse cells of early-stage *8131* germ-line clones are indistinguishable from those of the wild type, but after stage 5 *8131* germ-line clones remain in the five-blob configuration (**Fig. 1E and F**). The nurse-cell chromosomal dispersal defect is completely penetrant in *poly*<sup>2</sup> clones; all of the 66 stage-8 and stage-9 *poly*<sup>2</sup> germ-line clones examined maintained the nurse-cell dispersal defect.

To identify the target gene disrupted by the P-element in the *8131* line, we used inverse PCR to amplify the regions flanking the P-element; sequencing determined the site of insertion in the sole intron of the gene *poly* (naming based on Flybase nomenclature; **Fig. 1G**). This finding is supported by complementation analysis of the *8131* (designated *poly*<sup>2</sup>) allele with *poly*<sup>1</sup>, which also resides in the only intron of *poly*; *poly*<sup>2</sup> failed to complement *poly*<sup>1</sup>, resulting in decreased viability, similar to that of *poly*<sup>2</sup> homozygous mutants (**Table 1**). In addition, both *poly*<sup>2</sup> homozygous and *poly*<sup>1</sup>/*poly*<sup>2</sup> transheterozygous larvae exhibited delayed development, reaching third-instar and pupal stages later than their heterozygous siblings. To ensure that mutations in *poly* are responsible for the phenotypes seen in *poly*<sup>2</sup> germ-line clones, we performed rescue experiments in which we overexpressed *UASp-polyGFP* specifically in the germ-line with a *maternal- $\alpha$ -tubulin GAL4-VP16* (*mat-GAL4*) driver (**Fig. 2A**) in the background of *poly*<sup>2</sup> germ-line clones.<sup>17</sup> While the overexpression of PolyGFP may not reflect the endogenous localization of wild-type Poly, we have found PolyGFP to be ubiquitous in the germ-line and localized in nurse-cell nucleoplasm, as well as nurse-cell and oocyte cytoplasm. During midoogenesis, overexpression of PolyGFP was also enriched in the nurse-cell chromatin and oocyte cortex (**Fig. 2A**). Overexpression of PolyGFP in *poly*<sup>2</sup> germ-line clones fully alleviated Stau localization and nurse-cell chromosomal dispersal defects in all stage-9 and stage-10 egg chambers (**Fig. 2B–F**; *n* = 21), indicating that AP axis defects and nurse-cell chromosomal dispersal failure are caused by loss of *poly* function.

*poly* encodes a 251-amino-acid protein with no known domains. In an effort to deduce the function of *poly*, we used ClustalX to find putative homologs of *poly* in other model organisms (**Fig. 3**). Virtually identical *poly* coding sequences were found in all other *Drosophila* species; homologs in the *Aedes aegypti* mosquito and *Bombyx mori* silkworm show 53% and 47% sequence similarity, respectively, to *Drosophila melanogaster* Poly. The Poly protein sequence displays an extensive divergence from putative homologs from mammals, including *Homo sapiens* and *Mus musculus*, which retain 22–25% sequence identity and are known collectively as TMEM103 (transmembrane protein 103) or ATP1 (Angiotonin-transactivated protein 1) proteins and have unknown functions. The lengths of these proteins range from 211 to 256 amino acids, suggesting that, despite significant divergence between Poly and mammalian TMEM103 proteins, Poly still possesses similar functions in *Drosophila* species.

### ***poly* affects the localization of gurken and microtubule integrity**

To characterize further the involvement of *poly* in oocyte polarity, we examined the expression of Grk, a determinant of DV polarity of the egg chamber, in *poly*<sup>1</sup> and *poly*<sup>2</sup>

germ-line clones. Wild-type egg chambers displayed a dense localization of Grk at the dorsoanterior corner of the oocyte, tightly associated with the oocyte nucleus during stages 7–10 (**Fig. 4A**).<sup>8</sup> *poly*<sup>1</sup> and *poly*<sup>2</sup> stage-8 and stage-9 germ-line clones exhibited a weak Grk mislocalization phenotype (**Fig. 4B**), in which a small amount of Grk mislocalized to the ventral corner and/or aggregated into foci in the periphery of the oocyte nucleus. Although the Grk mislocalization phenotype was less pronounced than that in *hrb27C* and *sqd* mutants,<sup>11</sup> it was consistently present. Out of 67 stage-8 and stage-9 *poly*<sup>2</sup> germ-line clones examined, 42.4% showed wild-type Grk localization; 13.6% showed a reduced amount of Grk at the dorsoanterior corner of the oocyte, 27.3% showed some Grk foci, and 16.7% showed a trail of Grk toward the dorsoventral corner. The extent of Grk's effect on eggshell formation is not known, because both *poly*<sup>2</sup> mutant mothers and *poly*<sup>2</sup> germ-line-mutant mothers derived from the dominant female sterile technique both failed to deposit eggs.

Localization of Stau and Grk depends on an intact microtubule network in the germ-line cells. To determine the microtubule integrity in *poly* germ-line clones, we examined the localization of Kinesin:: $\beta$ -Galactosidase (Kin:: $\beta$ -Gal), a microtubule plus-end marker in the oocyte.<sup>18</sup> Kin:: $\beta$ -Gal in stage-9 wild-type egg chambers localized at the posterior of the oocyte (**Fig. 4C**). In *poly*<sup>2</sup> germ-line clones, Kin:: $\beta$ -Gal was frequently absent from the posterior or, occasionally, present in only low amounts, implying defective microtubule organization (**Fig. 4D**). Overall, our data suggest that *poly* is required in the germ-line for proper microtubule organization and oocyte polarity.

### ***poly* interacts with *hrb27C* and *otu***

*poly* germ-line clones display oogenic phenotypes reminiscent of some characterized members of the mRNP complex, including *hrb27C*. We therefore performed genetic-interaction experiments, using *hrb27C* alleles with *poly*<sup>2</sup> homozygous flies; *poly*<sup>1</sup> is fully recessive lethal, but *poly*<sup>2</sup> homozygous adults can be recovered and display many of the same oogenic phenotypes described above for *poly* germ-line clones (**Fig. 6A**). These studies did not produce conclusive results for ovarian phenotypes, because of the extremely small ovaries found in *poly*<sup>2</sup> homozygous mutants, but evidence of genetic interactions was revealed by modification of additional external phenotypes found in *poly* mutants. Specifically, *poly*<sup>2</sup> homozygotes and *poly*<sup>1</sup>/*poly*<sup>2</sup> transheterozygotes display notching of the wing margin, although the severity varies (**Fig. 5B**); P-element hop-outs of *poly*<sup>2</sup> yielded precise excision lines that showed intact wing-margins (data not shown). The wings of *hrb27C*<sup>377/+</sup> flies are wild-type in appearance (**Fig. 4C**), whereas a single copy of the *hrb27C*<sup>377</sup> mutation in the *poly*<sup>2</sup> homozygous mutant background strengthens the wing margin phenotype over that of *poly*<sup>2</sup> homozygosity alone (**Fig. 5D**). To ensure further that loss of *poly* caused the wing-margin loss in homozygous mutants, we successfully alleviated the wing-margin loss in *poly*<sup>2</sup> mutants by expressing a *UASpoly* transgene with the *actP-GAL4* driver (**Fig. 5E**).

On the basis of the wing-notching enhancement seen with reduction of *hrb27C* in the background of *poly*<sup>2</sup> homozygotes, we further studied the genetic interaction between *otu* and *poly*. The majority of alleles of identified mRNP components with germ-line functions phenocopy nurse-cell dispersal defects seen in heterozygous *otu*<sup>11</sup> and *otu*<sup>13</sup> mutants. Because mutations in a few of these components have been shown specifically to affect the Otu-104 kDa isoform, we performed genetic interaction studies with *otu* mutants and *poly*<sup>2</sup> germ-line clones. We detected no prominent changes in nurse-cell chromosomal dispersal in *otu*<sup>13/+</sup>; *poly*<sup>2</sup> germ-line clones (data not shown), but multiple copies of the *otu*-104 transgene facilitated further development of *poly*<sup>2</sup> homozygous ovaries. *poly*<sup>2</sup> mutant ovaries were small and displayed a wide variety of defects, including egg-chamber fusion, apoptosis and nurse-cell chromosome morphology defects (**Fig. 6A and B**). The

enhancement of phenotypes in *poly*<sup>2</sup> mutant egg chambers in comparison to *poly*<sup>2</sup> germline clones is most likely due to loss of Poly function in the somatic tissue in conjunction with loss of Poly in the germ-line, as induction of *poly*<sup>2</sup> follicleclones frequently undergo apoptosis (data not shown). In addition, *poly*<sup>1</sup>/*poly*<sup>2</sup> transheterozygotes and *poly*<sup>2</sup>/*Df6168* hemizygotes also presented similar defects in egg-chamber fusion and nurse-cell nuclei dispersal defects. In *poly*<sup>2</sup> mutant ovaries with four copies of the *otu-104* transgene, egg chambers progressed further in development, and the five-blob-configuration phenotype was rescued (**Fig. 6C**), but in *poly*<sup>2</sup> homozygous ovaries, nurse-cell chromosomal morphology defects persisted that were distinct from the five-blob configuration, and egg chamber fusion was still frequently seen (**Fig. 6C–F**). We conclude that *poly* functions downstream of *otu* and those higher levels of the Otu-104 kDa protein can partially suppress *poly* phenotypes.

## Discussion

In addition to *hrb27C*, *sqd* and *pUf68*, mutations in genes encoding transcription factors E2F1 and DP, the chromo-domain protein Rhino, the RNA helicase P68, and Spoonbill all affect nurse-cell chromosome dispersal and *grk* mRNA localization.<sup>19–23</sup> Similar ovarian phenotypes displayed in mutants for these genes suggest a significant spatiotemporal link between nurse-cell chromosomal organization and oocyte polarity. The great functional diversity represented by these genes highlights the complexity of this essential yet poorly understood process. Here, we report that the novel gene, *poly*, is required for nurse-cell chromosome dispersal and AP/DV polarity. Our evidence of genetic interactions among *poly*, *hrb27C* and *otu* suggests that Poly is involved in processes similar to those of these previously characterized proteins. The *otu-104* transgene (containing a large genomic fragment of *otu* that contains exon 6a) alleviates the *Grk* mislocalization and nurse-cell chromosome-dispersal failure defects of *pUf68*, *sqd* and *hrb27C*.<sup>11</sup> Overexpression of Otu-104 partially rescues the *poly* mutant ovarian phenotypes, but the persistent fusion of egg chambers and nurse-cell nuclear defects in this rescue experiment suggest that *poly* mutations affect the expression of additional genes that mediate nurse-cell chromosome architecture and oocyte polarity formation/maintenance.

The interactions among different members of the mRNP complexes in *Drosophila* oogenesis cataloged to date are either protein-protein (such as *cup-eIF4E*)<sup>24</sup> or RNA-dependent (*hrb27C-sqd*).<sup>11</sup> The lack of any known protein domains in Poly prevents formation of a clear idea of Poly's possible functions in *Drosophila* oogenesis. From our results, we conclude that *poly* mutations affect the expression of genes independently or downstream of *otu*. Further studies are needed that can reveal the molecular mechanisms of *poly* and can identify the downstream targets that are affected by loss of *poly* function.

## Methods

### Fly stocks

Fly stocks bearing the following mutations were used: *poly*<sup>11648</sup> (a P-element insertion allele from the Bloomington stock center that was recombined to the FRT82B chromosome; designated *poly*<sup>1</sup>) [FBal0035465], *poly*<sup>2</sup> (known as P-element insertion 8131; from the Szeged stock center, Hungary) [FBal0190755], P[otu-104] (*ovarian tumor* 104-kDa isoform on the third chromosome, a gift from Dr. Lillian Searles; on the second chromosome, a gift from Dr. Trudi Schupbach) [FBtp0004944]. The *kin-lacZ* line (a gift from Dr. Hannele Ruohola-Baker)<sup>18</sup> [FBti0002915] was used to determine the integrity of microtubules in *poly* germ-line clones. Although it is not known if *poly*<sup>1</sup> is a null allele, the complete larval lethality of the *poly*<sup>1</sup> line, as well as the difficulty in creation of stage-9 *poly*<sup>1</sup> germ-line clones, allows classification of *poly*<sup>2</sup> as a hypomorph allele.



To generate *poly* germ-line clones, we used hsFLP,  $\alpha$ Tub67C-GFP-Stau;<sup>25,26</sup> FRT82B ubi-GFP/TM6B Hu Tb or TM3 Sb, and hsFLP; FRT82BarmlacZ/TM6B Hu Tb stocks (original FRT82B-ubiGFP and FRT82BarmLacZ stocks with FBIDs FBst0005188 and FBst0008218, respectively). For overexpression of *poly*, a full length cDNA, kindly supplied by Dr. Margarete Heck, was cloned into a pUASp vector by the FSU Molecular Cloning Facility, with or without the eGFP tag at the amino terminus, and injected into embryos according to standard procedures (performed by Duke University Model System Genomics). The P[mat- $\alpha$ -tubulin-GAL4VP16] driver [FBst0007062] on the second chromosome was used for germ-line-specific overexpression of *poly*. The P[actin-GAL4] driver [FBst0004414] on the second chromosome was used for ubiquitous overexpression of *poly*.

### ***poly* population analysis**

Multiple vials of *poly*<sup>2</sup> stocks were expanded, transferred repeatedly, and kept at 18°C, 25°C or 29°C for population analysis of *poly*<sup>2</sup> homozygotes for one generation. Multiple vials of *poly*<sup>1</sup> flies crossed to *poly*<sup>2</sup> flies were given identical experimental treatment and examined for the presence of *poly*<sup>1</sup>/*poly*<sup>2</sup> transheterozygotes for one generation as well. The percentage of viability was defined as the actual number of *poly* mutant flies scored, divided by the expected number of *poly* mutant flies, which is half of the number of balanced siblings. SE stands for standard (sampling) error and is related to standard deviation, i.e., the probability that data collected from the sample size is inaccurate. For the standard error of *poly* homozygote/transheterozygote viability, the following formula was used:

$$(SE=SD \text{ (standard deviation) of sample}) / (\text{square root of } n \text{ (total sample size)})$$

where the standard deviation for 1 out of the 4 possible genotypic classes of progeny is the square root of  $(0.25 \times 0.75)$ , approximately 0.433.<sup>31</sup> Subsequent calculation of the standard error from standard-deviation values demonstrated that the smaller the SE value was, the more statistically significant the data collected from the sample size was; this result provides additional evidence that the sample size was adequate to demonstrate temperature-sensitive viability in *poly* homozygotes/transheterozygotes.

### **Generation of mosaic clones by the FLP-FRT technique**

Fly crosses and rearing were performed under standard conditions.<sup>27</sup> The FLP-FRT system was used to induce mitotic recombination and produce clones in the ovary through the heat-shock flipase (hsFLP) on the X chromosome. To obtain germ-line clones, we heat shocked second- and third-instar larvae for 2 hours on two consecutive days; the larvae were then reared at 25°C for eight days, sorted and moved to fresh vials with yeast for two additional days before dissection.<sup>28</sup> Clones were marked by the absence of ubi-GFP<sup>29</sup> or arm-lacZ.

### **Genetic interaction studies**

*hrb27C*<sup>377</sup> (located on the second chromosome) was crossed to a Sp/CyO; *poly*<sup>2</sup>/TM6B stock and crossed to *poly*<sup>2</sup>/TM6B again to produce *poly*<sup>2</sup> escapers with heterozygous loss of *hrb27C* in the background. Progeny were reared at 18°C, a temperature that maximized number of escapers for study.

### **Inverse PCR**

Inverse PCR was performed according to the standard BDGP protocol with primers for amplifying flanking sequences of the P{LacW} element. Recovery of flanking sequence data for the *8131* insertion revealed the insertion in the sole intron of the *poly* gene.

## Immunocytochemistry

Immunocytochemistry was performed under standard conditions.<sup>30</sup> The antibodies used were mouse anti-Gurken (1:20; Developmental Studies Hybridoma Bank), rabbit anti-Staufen (1:2,000; a gift from D. St. Johnston), and mouse anti- $\beta$ -galactosidase G4644 at 1:1,000 dilution (Sigma-Aldrich).

## Multiple alignment analysis

*poly* coding sequences from other species of *Drosophila* and putative homologues from nondipteran species were aligned with ClustalX 2.0.10 and modified in Adobe Photoshop CS2.

## Acknowledgments

We thank Anne B. Thistle, Jamila Horabin and Yoichiro Tamori for critical reading and helpful input into the manuscript; Margarete Heck for sharing reagents before publication and for critical reading of the manuscript; Trudi Schupbach for *hrb27C* mutants; Lillian Searles for the *otu-104* transgene; Daniel St. Johnston for *staufen* antibodies; the Molecular Cloning Lab (Michael Asher, Rani Dhanarajan, Andre Irsigler) at Florida State University for cloning of the *poly* gene into the UASp vector; and Kimberly Riddle and the FSU Biological Science Imaging Resource facility for assistance with electron microscopy and confocal imaging. We also thank David Houle and his lab for assistance with wing imaging; Chris Green, Amanda Novak and Yi-Chun Huang for stock maintenance and food preparation; Andrea Bixler for assistance in experiments; and Jianjun Sun, Laila Smith and John Poulton for discussion and interpretation of results and for critical reading of the manuscript. W.-M. Deng is supported by a National Institutes of Health grant R01 GM072562.

## Abbreviations

<b>armLacZ</b>	<i>armadillo-lacZ</i>
<b>eGFP</b>	enhanced GFP
<b>GFP</b>	green fluorescent protein
<b>Hu</b>	humeral (marker)
<b>kDa</b>	kilodalton
<b>PCR</b>	polymerase chain reaction
<b>Sb</b>	stubble (marker)
<b>TM3</b>	third multiple three (balancer)
<b>TM6B</b>	third multiple six, B structure (balancer)
<b>Tb</b>	tubby (marker)
<b>UASp</b>	upstream activation sequence P-element construct
<b>ubi-GFP</b>	<i>ubiquitin</i> -GFP

## References

1. Cooley L, Theurkauf WE. Cytoskeletal functions during *Drosophila* oogenesis. *Science*. 1994; 266:590–6. [PubMed: 7939713]
2. Spradling, AC., editor. Developmental genetics of oogenesis. Cold Spring Harbor Laboratory Press; New York: 1993.
3. Riechmann V, Ephrussi A. Axis formation during *Drosophila* oogenesis. *Curr Opin Genet Dev*. 2001; 11:374–83. [PubMed: 11448623]
4. Steinhauer J, Kalderon D. Microtubule polarity and axis formation in the *Drosophila* oocyte. *Dev Dyn*. 2006; 235:1455–68. [PubMed: 16586443]

5. Theurkauf WE, Smiley S, Wong ML, Alberts BM. Reorganization of the cytoskeleton during *Drosophila* oogenesis: implications for axis specification and inter-cellular transport. *Development*. 1992; 115:923–36. [PubMed: 1451668]
6. St. Johnston D, Beuchle D, Nusslein-Volhard C. Staufen, a gene required to localize maternal RNAs in the *Drosophila* egg. *Cell*. 1991; 66:51–63. [PubMed: 1712672]
7. Brendza RP, Serbus LR, Duffy JB, Saxton WM. A function for kinesin I in the posterior transport of oskar mRNA and Staufen protein. *Science*. 2000; 289:2120–2. [PubMed: 11000113]
8. Neuman-Silberberg FS, Schupbach T. The *Drosophila* dorsoventral patterning gene *gurken* produces a dorsally localized RNA and encodes a TGF $\alpha$ -like protein. *Cell*. 1993; 75:165–74. [PubMed: 7691414]
9. Poulton JS, Deng WM. Cell-cell communication and axis specification in the *Drosophila* oocyte. *Dev Biol*. 2007; 311:1–10. [PubMed: 17884037]
10. Van Buskirk C, Schupbach T. Half pint regulates alternative splice site selection in *Drosophila*. *Dev Cell*. 2002; 2:343–53. [PubMed: 11879639]
11. Goodrich JS, Clouse KN, Schupbach T. Hrb27C, Sqd and Otu cooperatively regulate *gurken* RNA localization and mediate nurse cell chromosome dispersion in *Drosophila* oogenesis. *Development*. 2004; 131:1949–58. [PubMed: 15056611]
12. Huynh JR, Munro TP, Smith-Litière K, Lepesant JA, St. Johnston D. The *Drosophila* hnRNP A/B homolog, Hrp48, is specifically required for a distinct step in *osk* mRNA localization. *Dev Cell*. 2004; 6:625–35. [PubMed: 15130488]
13. Dej KJ, Spradling AC. The endocycle controls nurse cell polytene chromosome structure during *Drosophila* oogenesis. *Development*. 1999; 126:293–303. [PubMed: 9847243]
14. Deak P, Omar MM, Saunders RD, Pal M, Komonyi O, Szidonya J, et al. P-element insertion alleles of essential genes on the third chromosome of *Drosophila melanogaster*: correlation of physical and cytogenetic maps in chromosomal region 86E-87F. *Genetics*. 1997; 147:1697–722. [PubMed: 9409831]
15. Bellotto M, Bopp D, Senti KA, Burke R, Deak P, Maroy P, et al. Maternal-effect loci involved in *Drosophila* oogenesis and embryogenesis: P element-induced mutations on the third chromosome. *Int J Dev Biol*. 2002; 46:149–57. [PubMed: 11902676]
16. Lopez-Schier H, St. Johnston D. Delta signaling from the germ line controls the proliferation and differentiation of the somatic follicle cells during *Drosophila* oogenesis. *Genes Dev*. 2001; 15:1393–405. [PubMed: 11390359]
17. Rorth P. Gal4 in the *Drosophila* female germline. *Mech Dev*. 1998; 78:113–8. [PubMed: 9858703]
18. Clark IE, Jan LY, Jan YN. Reciprocal localization of Nod and kinesin fusion proteins indicates microtubule polarity in the *Drosophila* oocyte, epithelium, neuron and muscle. *Development*. 1997; 124:461–70. [PubMed: 9053322]
19. Volpe AM, Horowitz H, Grafer CM, Jackson SM, Berg CA. *Drosophila* rhino encodes a female-specific chromo-domain protein that affects chromosome structure and egg polarity. *Genetics*. 2001; 159:1117–34. [PubMed: 11729157]
20. Royzman I, Hayashi-Hagihara A, Dej KJ, Bosco G, Lee JY, Orr-Weaver TL. The E2F cell cycle regulator is required for *Drosophila* nurse cell DNA replication and apoptosis. *Mech Dev*. 2002; 119:225–37. [PubMed: 12464435]
21. Motola S, Neuman-Silberberg FS. Spoonbill, a new *Drosophila* female-sterile mutation, interferes with chromosome organization and dorsal-ventral patterning of the egg. *Dev Dyn*. 2004; 230:535–45. [PubMed: 15188438]
22. Buszczak M, Spradling AC. The *Drosophila* P68 RNA helicase regulates transcriptional deactivation by promoting RNA release from chromatin. *Genes Dev*. 2006; 20:977–89. [PubMed: 16598038]
23. Neuman-Silberberg FS. *Drosophila* female sterile mutation spoonbill interferes with multiple pathways in oogenesis. *Genesis*. 2007; 45:369–81. [PubMed: 17492752]
24. Nakamura A, Sato K, Hanyu-Nakamura K. *Drosophila* cup is an eIF4E binding protein that associates with Bruno and regulates oskar mRNA translation in oogenesis. *Dev Cell*. 2004; 6:69–78. [PubMed: 14723848]



25. Schuldt AJ, Adams JH, Davidson CM, Micklem DR, Haseloff J, St. Johnston D, Brand AH. Miranda mediates asymmetric protein and RNA localization in the developing nervous system. *Genes Dev.* 1998; 12:1847–57. [PubMed: 9637686]
26. Martin SG, Leclerc V, Smith-Litière K, St. Johnston D. The identification of novel genes required for *Drosophila* anteroposterior axis formation in a germline clone screen using GFP-Staufen. *Development.* 2003; 130:4201–15. [PubMed: 12874138]
27. Poulton JS, Deng WM. Dystroglycan downregulation links EGF receptor signaling and anterior-posterior polarity formation in the *Drosophila* oocyte. *Proc Natl Acad Sci USA.* 2006; 103:12775–80. [PubMed: 16908845]
28. Deng WM, Ruohola-Baker H. Laminin A is required for follicle cell-oocyte signaling that leads to establishment of the anterior-posterior axis in *Drosophila*. *Curr Biol.* 2000; 10:683–6. [PubMed: 10837250]
29. Maines JZ, Stevens LM, Tong X, Stein D. *Drosophila* dMyc is required for ovary cell growth and endoreplication. *Development.* 2004; 131:775–86. [PubMed: 14724122]
30. Deng WM, Althausen C, Ruohola-Baker H. Notch-Delta signaling induces a transition from mitotic cell cycle to endocycle in *Drosophila* follicle cells. *Development.* 2001; 128:4737–46. [PubMed: 11731454]
31. Freedman, D.; Pisani, R.; Purves, R. *Statistics*. 1st edn.. Norton; New York: 1978.

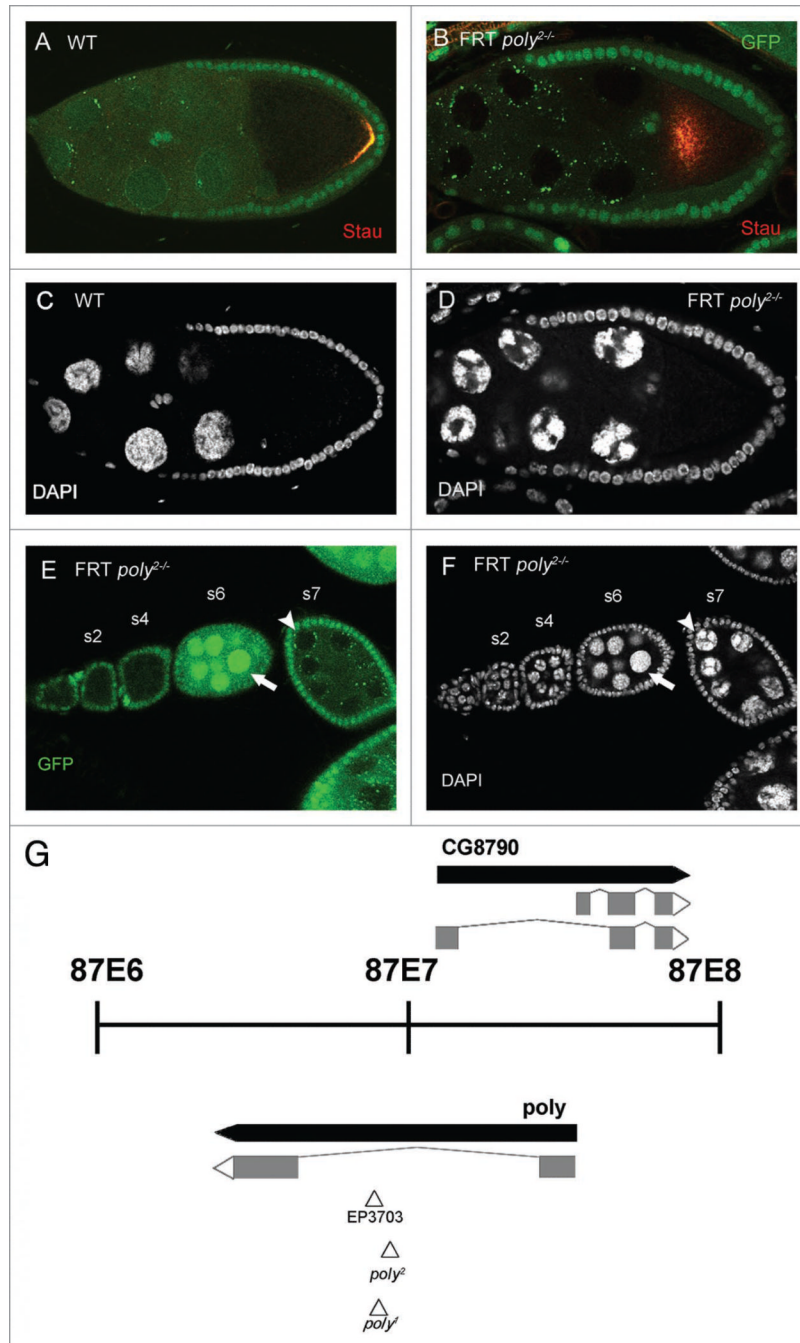


**Figure 1.**

The identification of the novel gene *poly* isolated by a flipase-flipase recognition-target mosaic screen for mutations affecting anteroposterior axis polarity. (A) In wild-type stage-9 egg chambers, *stau* is localized at the posterior of the oocyte, and nurse-cell chromosome morphology is diffuse (c). (B) *stau* localization is disrupted in the majority of *poly*<sup>2</sup> germ-line clones; complete mislocalization of *stau* is seen in the center of the oocyte, and nurse-cell chromosomes fail to disperse (D). The wild-type ovariole displays a polytenic configuration in the very early stages before rearrangement to a five-blob configuration that precedes dispersal to a diffuse state in stages 5–6 of oogenesis (early stages at the anterior/left and later stages at the posterior/right). (e and F) An ovariole that contains *poly*<sup>2</sup> germ-

line clones, early stages at the anterior/left and later stages at the posterior/right. *poly*<sup>2</sup> germ-line clones, before stage 5, are indistinguishable from wild-type polytenic configurations. The wild-type egg chamber that precedes the posteriormost germ-line clone has dispersed nurse-cell chromosomes (arrow), whereas the germ-line clone maintains a five-blob configuration, indicating a failure to disperse (arrowhead). (G) *poly* is a partially nested novel gene that encodes a 251-amino-acid protein and has been cytologically mapped to the 87e region. All three p-elements are inserted in close proximity to each other in the sole intron of *poly*.

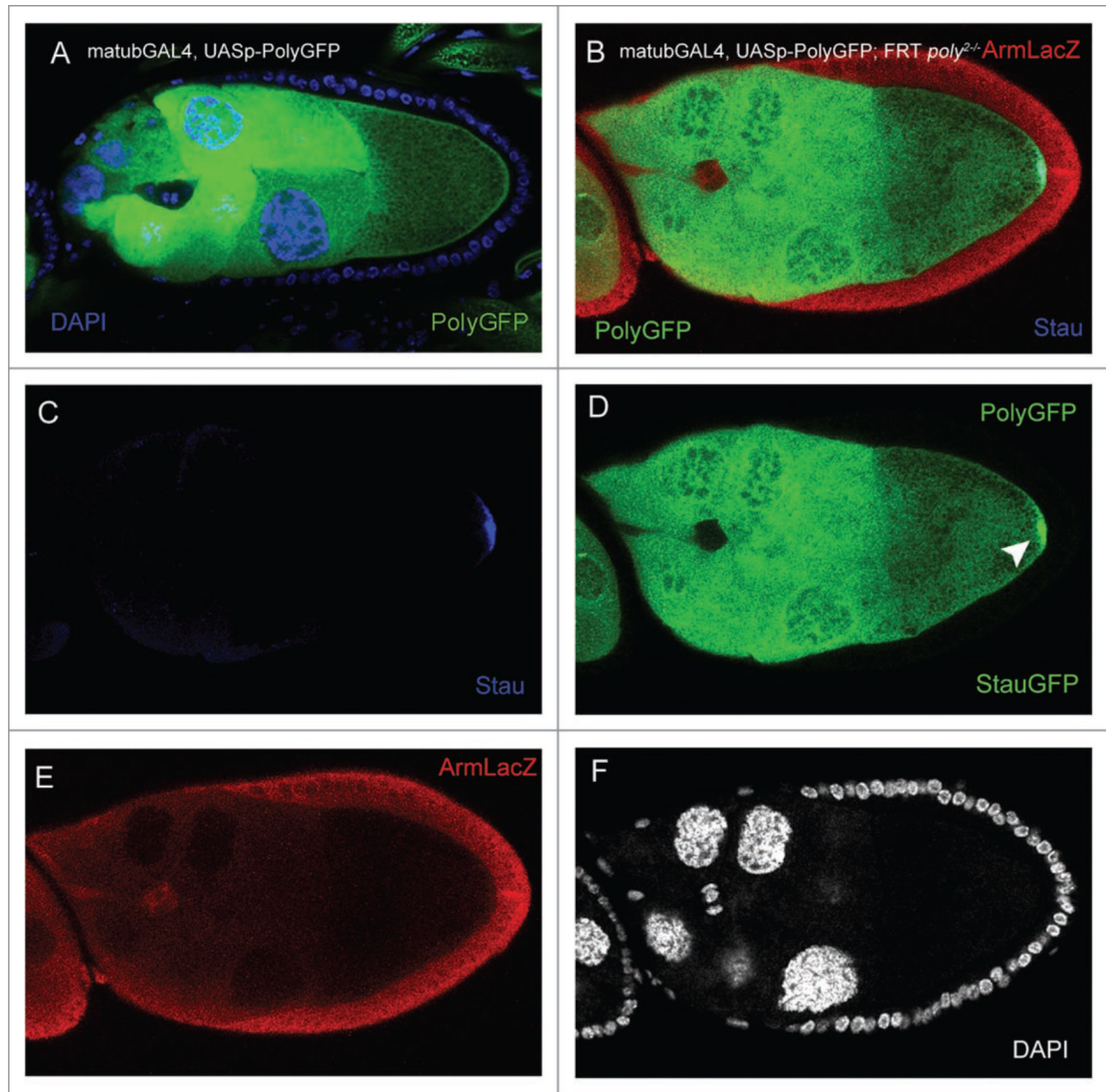


**Figure 2.**

In *poly* germ-line clones, *stau* localization and nurse-cell chromosome-dispersal are affected and are rescued by germ-line-specific over-expression of UASp-*polyGFP*. (A) Overexpression of UASp-*polyGFP* transgene with the *mat*-GAL4 driver in a stage-9 egg chamber reveals ubiquitous expression of polyGFP in the nurse-cell nuclei and cytoplasm, as well as the oocyte, with enrichment around the oocyte cortex. Overexpression of polyGFP frequently causes a modest granulation of the nurse-cell nuclei in ovaries from older females. (B) Overexpression of UASp-*polyGFP* in the background of *poly*<sup>2</sup> germ-line clones fully alleviates the five-blob-arrest phenotype and *stau* mislocalization. (c) *stau* is localized to the posterior of the oocyte. (D) UASp-*polyGFP* overexpression in the egg chamber, with concurrent *stau*-GFP localization at the posterior of the oocyte (arrowhead). polyGFP protein is not enriched at the posterior of the oocyte. (e) Germ-line clone marked by the absence of arm-lacZ. (F) DAPI channel revealing the diffuse nature of the nurse-cell chromosomes.



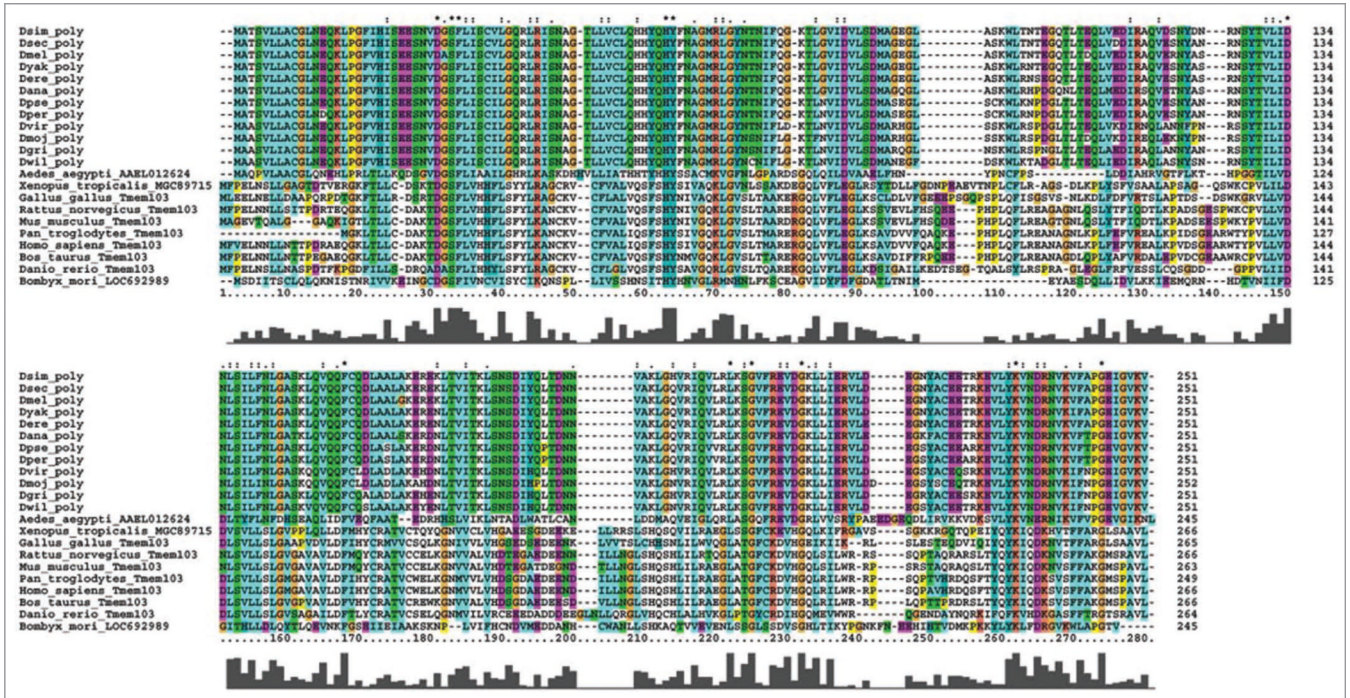


**Figure 3.** Clustalx alignment of *poly* with putative homologues. *Drosophila melanogaster poly* is virtually identical to homologues in other drosophilids and displays moderate sequence homology to those in other insect species; it diverges most greatly from mammalian homologues. each protein sequence is labeled by genus and species and the name of the protein; for drosophilids, the genus is denoted as D and the first three letters of the species name are added. In the alignment, the bar graph under each amino acid delineates the conservation of that amino acid in the alignment of all protein sequences.



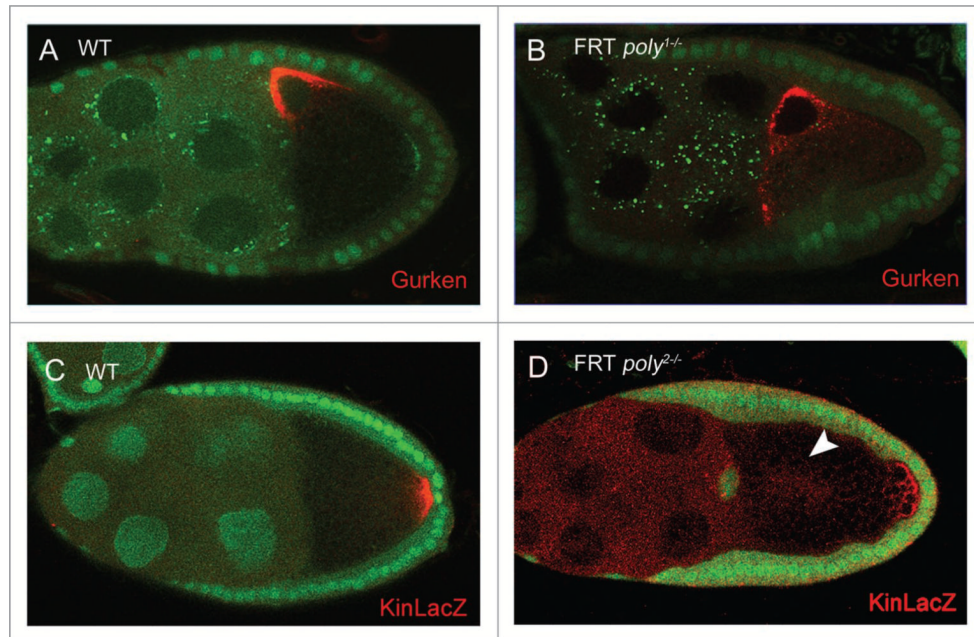


**Figure 4.**

In *poly* germ-line clones, Grk and kin-lacZ localization are affected during oogenesis. (A) Grk is localized at the dorsoanterior corner of the oocyte in wild-type stage-8 and stage-9 egg chambers. (B) *poly<sup>1</sup>* stage-8 and stage-9 germ-line clones display weak Grk mislocalization that consists of trails of Grk protein to the ventral corner. (c) Kinesin also localizes at the posterior of the oocyte in wild-type stage-9 egg chambers, as evidenced by kin-lacZ staining. (D) In *poly<sup>2</sup>* stage-9 germ-line clones, Kin:: $\beta$ -gal localization is also disrupted, and Kin:: $\beta$ -gal levels are occasionally reduced (arrowhead points to mislocalized Kin:: $\beta$ -gal in the center of the oocyte).

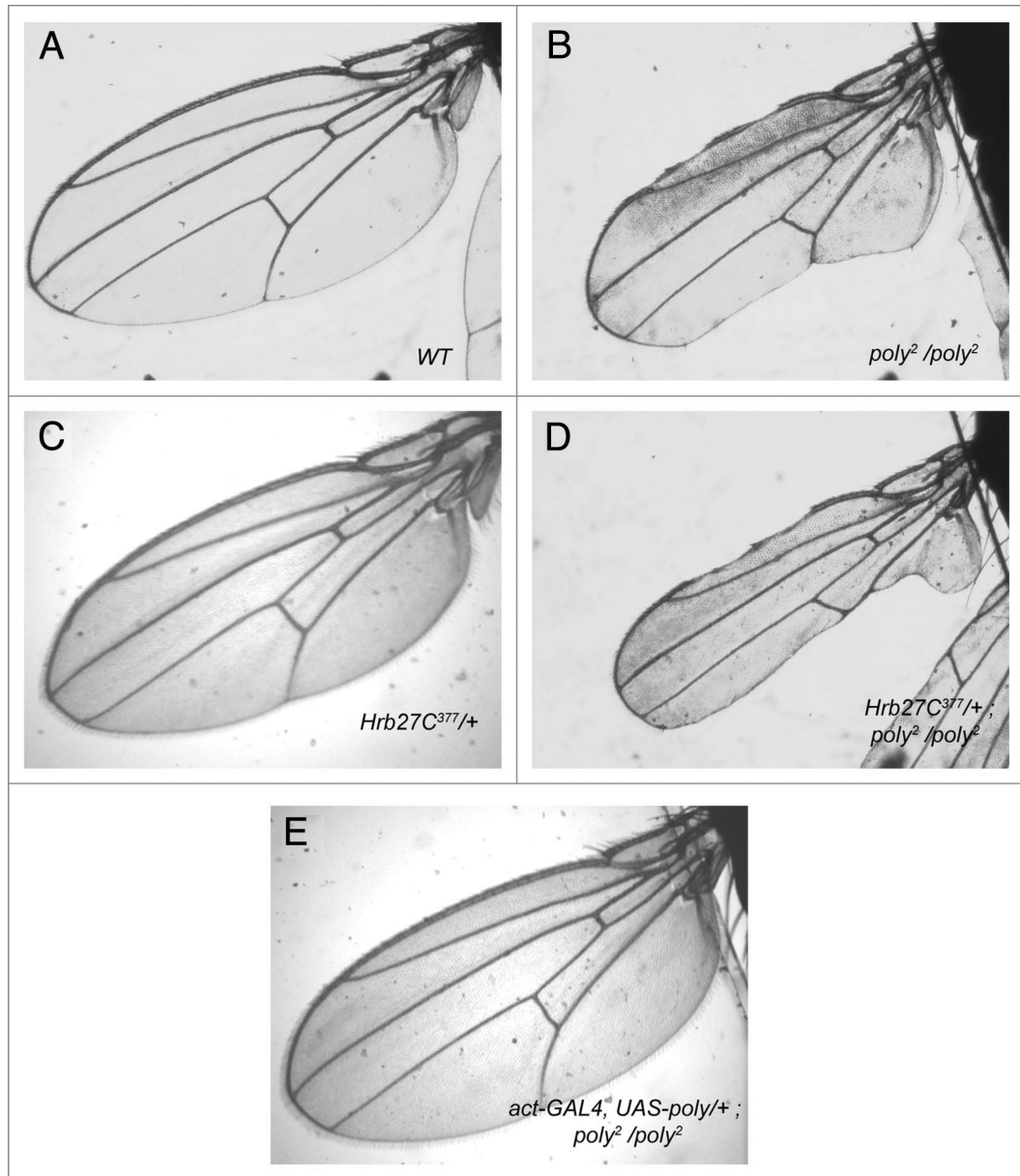


**Figure 5.**

The wing-margin-loss phenotype of  $poly^2$  mutant adults is strengthened by reduction of *hrb27C*. (A) Light microscopy of a wild-type *Drosophila melanogaster* wing. (B) Variable wing-margin loss is present in all  $poly^2/poly^2$  escapers. (c)  $hrb27C^{377/+}$  flies show no defects in the wing margins. (D) A single copy of the  $hrb27C^{377}$  mutation strengthens the wing-margin loss of  $poly^2$  homozygotes. (e) Overexpression of UAS-*poly* with the *act-GAL4* driver in the background of  $poly^2$  mutant flies alleviates the wing-margin loss defect.

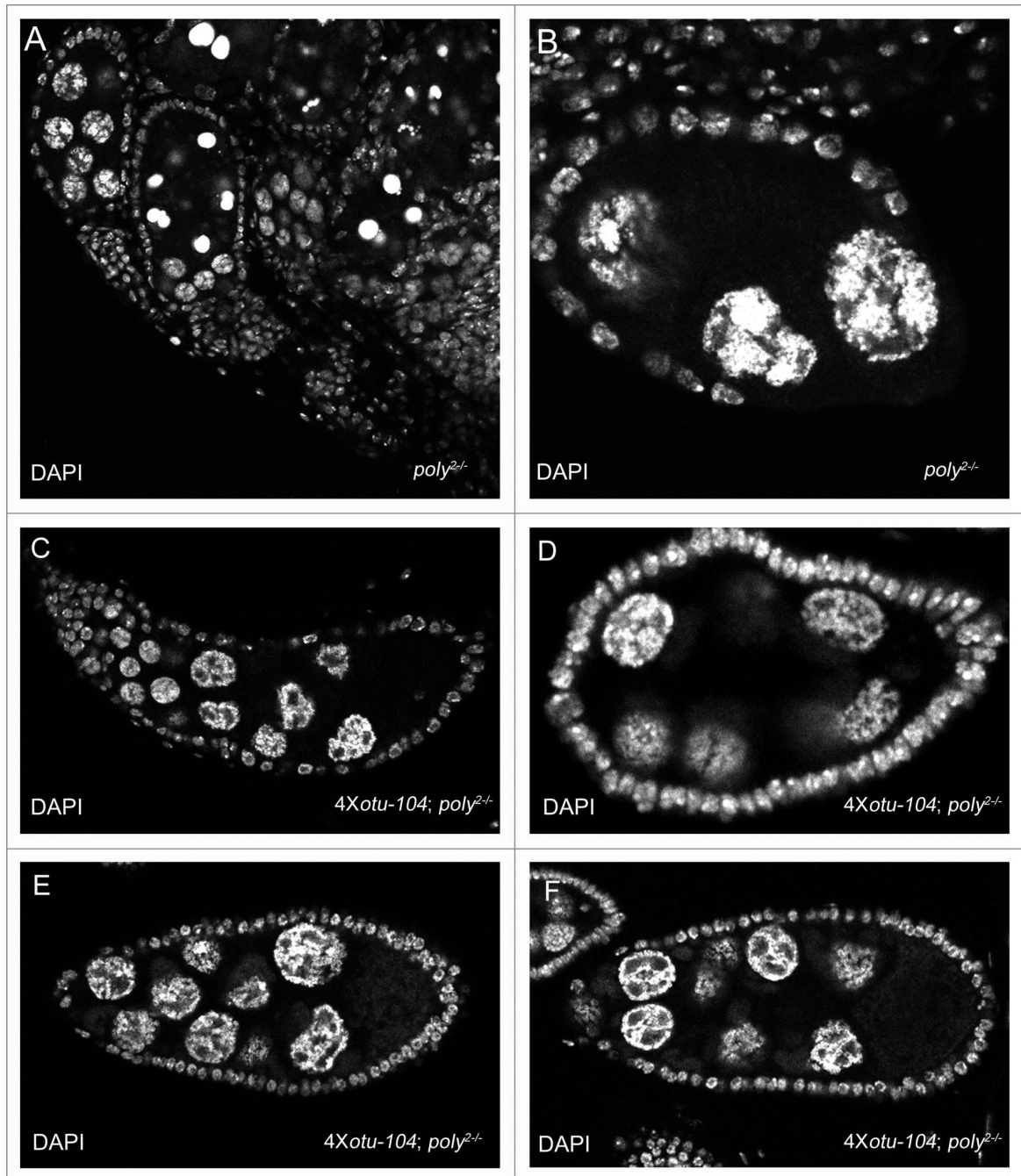


**Figure 6.**

Multiple copies of the *otu-104* transgene can partially rescue *poly<sup>2</sup>* mutant ovaries. (A) *poly<sup>2</sup>* mutant ovary displaying apoptosis, egg chamber fusion, and nurse-cell chromosome morphology defects. (B) *poly<sup>2</sup>* egg chamber retaining the five-blob configuration in the nurse-cell nuclei. (C) egg chamber fusion of multiple egg chambers in a *poly<sup>2</sup>* ovariole with overexpression of Otu-104. (D) stage-6 4x *otu-104*, *poly<sup>2</sup>* mutant egg chamber displaying nurse-cell chromosomal abnormalities distinct from the five-blob configuration. (E and F) Rare stage-8 and stage-9 *poly<sup>2</sup>* egg chambers with overexpression of Otu-104 with granulated nurse-cell morphology defects.

**Table 1**

Analysis of the temperature sensitivity of *poly<sup>2</sup>/poly<sup>2</sup>* and *poly<sup>1</sup>/poly<sup>2</sup>* mutant flies

Rearing temperature	<i>poly<sup>2</sup>/poly<sup>2</sup></i>	<i>poly<sup>2</sup>/TM3</i>	Percentage of viability	% SE	Total
18°C	347	4751	14.6%	0.61%	5098
25°C	9	1085	1.66%	1.31%	1094
29°C	0	636	0%	1.98%	636

Rearing temperature	<i>poly<sup>1</sup>/poly<sup>2</sup></i>	<i>poly<sup>1</sup> or poly<sup>2</sup>/TM3</i>	Percentage of viability	% SE	Total
18°C	205	1474	27.8%	1.06%	1679
25°C	80	469	34.1%	1.85%	549
29°C	0	204	0%	3.03%	204

Viability of *poly* homozygous escapers is low at 18°C, decreases further with increasing temperature, and is zero at 29°C. *poly* transheterozygous escapers are more viable than their homozygous counterparts at the intermediate temperature (possibly as a result of intragenic complementation) but still do not survive at 29°C. % SE is related to the standard deviation of the sample and is the sampling error, i.e., the probability that data obtained from the sample size is inaccurate.